TITLE:

Effective precondition technique to solve a full linear system for the fast multipole method

AUTHOR(S):

Hamada, S; Takuma, T

CITATION:

Hamada, S ...[et al]. Effective precondition technique to solve a full linear system for the fast multipole method. IEEE TRANSACTIONS ON MAGNETICS 2003, 39(3): 1666-1669

ISSUE DATE:

2003-05

URL:

http://hdl.handle.net/2433/39999

RIGHT:

(c)2003 IEEE. Personal use of this material is permitted. However, permission to reprint/republish this material for advertising or promotional purposes or for creating new collective works for resale or redistribution to servers or lists, or to reuse any copyrighted component of this work in other works must be obtained from the IEEE.

京都大学学術情報リポジトリ
KURENAI
Kyoto University Research Information Repository

京都大学 KYOTO UNIVERSITY
A Self-archived copy in
Kyoto University Research Information Repository
https://repository.kulib.kyoto-u.ac.jp
京都大学学術情報リポジトリ KURENAI 紅 Kyoto University Research Information Repository

Effective Precondition Technique to Solve a Full Linear System for the Fast Multipole Method

Shoji Hamada, *Member, IEEE,* and Tadasu Takuma, *Fellow, IEEE*

***Abstract*—The fast multipole method (FMM) is an $O(N)$ solver of a full linear system appearing in integral equation methods. We propose a precondition technique for the FMM using the Bi-CGSTAB2 method, which employs a nested FMM having intentionally deteriorated precision. This enables us to utilize the global information residing in the system matrix.**

***Index Terms*—Boundary element methods, fast multipole method (FMM), iterative methods, Laplace equations, precondition.**

I. Introduction

INTEGRAL equation methods need to solve a full $N \times N$ linear system, $A\boldsymbol{x} = \boldsymbol{b}$, that appears in a field calculation problem. The fast multipole method (FMM) [1], [2] is an $O(N)$ algorithm to calculate the product of A and an arbitrary vector $\boldsymbol{x}_{\rm arb}$, $A\boldsymbol{x}_{\rm arb}$, which is used to solve $\boldsymbol{x} = A^{-1}\boldsymbol{b}$ by an iterative solver such as the Bi-CGSTAB2 method [3] that we use here. In the FMM, $A\boldsymbol{x}_{\rm arb}$ is calculated separately as the sum of a near part and a far part, that is, $A_{\rm near}\boldsymbol{x}_{\rm arb} + A_{\rm far}\boldsymbol{x}_{\rm arb}$. Application of ILU(0) is the most popular precondition technique for the FMM [4], where $A_{\rm near}$ is stored and used as an approximation of A ($A_{\rm appx}$). Although ILU(0) accelerates the convergence of iteration, it requires a lot of memory because it has to store both the matrix LU and ${A_{\rm near}}^{\rm str}$, where "str" indicates storage in memory. Furthermore, the acceleration performance of ILU(0) is not always satisfactory because of its rough approximation of A by $A_{\rm near}$.

II. Precondition by Nested FMM

An iterative solver requires a procedure to calculate $A\boldsymbol{x}_{\rm arb}$ to solve $\boldsymbol{x} = A^{-1}\boldsymbol{b}$ at every (major) iteration step. A second requirement of an iterative solver is a procedure to calculate ${A_{\rm appx}}^{-1}\boldsymbol{b}_{\rm arb}$ to accelerate its convergence. The latter is called precondition. We propose to solve ${A_{\rm appx}}^{-1}\boldsymbol{b}_{\rm arb}$ by a nested, or minor, iterative solver that is the same as or similar to the major one without precondition. This nested solver needs only a procedure to calculate $A_{\rm appx}\boldsymbol{x}_{\rm arb}$. This method, which we call the minor iterative precondition (MIP), may be meaningless when the matrix A is sparse. But when A is full, the "major" step takes much more time than the minor one, thus making MIP meaningful. The most significant merit of the MIP is that it can employ some kinds of $A_{\rm appx}$ that are different from $A_{\rm near}$, such as the following:

$$A_{\rm appx}\boldsymbol{x}_{\rm arb} = {A_{\rm near}}^{\rm str}\boldsymbol{x}_{\rm arb} + {A_{\rm far}}^{\rm DP}\boldsymbol{x}_{\rm arb} \quad (1)$$

$$A_{\rm appx}\boldsymbol{x}_{\rm arb} = {A_{\rm near}}^{\rm DP}\boldsymbol{x}_{\rm arb} + {A_{\rm far}}^{\rm DP}\boldsymbol{x}_{\rm arb} \quad (2)$$

where DP refers to a calculation by a nested or minor FMM having intentionally deteriorated precision, thus being many orders faster than the major FMM. These equations roughly include $A_{\rm far}$, that is, they offer global approximations of A. Thus, they are expected to significantly accelerate the convergence of the major iterative solver.

The proposed simple concept that a nested FMM provides an effective preconditioner can be a general technique for many kinds of linear problems using the FMM.

III. Electrostatic Field Calculation by the Boundary Element Method

In order to examine the performance of the proposed precondition technique, we treat the boundary element method (BEM) that analyzes electrostatic field problems in piecewise homogeneous dielectrics. When a closed region B with permittivity ε_B exists in the open region A with ε_A, a boundary potential u_i is represented by the following integral equations:

$$c_i^A u_i = \int_S \frac{\frac{D_n}{\varepsilon_A}}{4\pi|\boldsymbol{r}|}dS + \int_S \frac{u}{4\pi|\boldsymbol{r}|^2}\left(\frac{\boldsymbol{r}}{|\boldsymbol{r}|}\cdot\boldsymbol{n}\right)dS + u_{i0} \quad (3)$$

$$c_i^A = \int_s \frac{1}{4\pi|\boldsymbol{r}|^2}\left(\frac{\boldsymbol{r}}{|\boldsymbol{r}|}\cdot\boldsymbol{n}\right)dS + 1 \quad (4)$$

$$c_i^B u_i = -\int_S \frac{\frac{D_n}{\varepsilon_B}}{4\pi|\boldsymbol{r}|}dS - \int_s \frac{u}{4\pi|\boldsymbol{r}|^2}\left(\frac{\boldsymbol{r}}{|\boldsymbol{r}|}\cdot\boldsymbol{n}\right)dS \quad (5)$$

$$c_i^B = -\int_S \frac{1}{4\pi|\boldsymbol{r}|^2}\left(\frac{\boldsymbol{r}}{|\boldsymbol{r}|}\cdot\boldsymbol{n}\right)dS \quad (6)$$

where S is the boundary surface between A and B, D_n and u are the normal component of the dielectric flux density and the potential on dS, respectively, $\boldsymbol{n}$ is the outward normal vector of dS, $\boldsymbol{r}$ is the position vector from dS to the position of u_i, and u_{i0} is the potential by an infinite source, that is, by an applied field. The first and second terms of (3) and (5) have the same forms as a point charge potential and a dipole charge potential, respectively.

When the S is discretized by boundary elements and the M unknowns respectively represent D_n and u, then $2M = N$ equations of (3) and (5) at M node points give a full linear matrix to solve the unknowns.

Manuscript received June 18, 2002.

S. Hamada is with the Department of Electrical Engineering, Kyoto University, Kyoto 606-8501, Japan (e-mail: shamada@ kuee.kyoto-u.ac.jp).

T. Takuma is with the Central Research Institute of Electric Power Industry (CRIEPI), Tokyo 201-8511, Japan (e-mail: takuma@criepi.denken.or.jp).

Digital Object Identifier 10.1109/TMAG.2003.810335

0018-9464/03$17.00 © 2003 IEEE

京都大学 KYOTO UNIVERSITY
A Self-archived copy in
Kyoto University Research Information Repository
https://repository.kulib.kyoto-u.ac.jp
京都大学学術情報リポジトリ KURENAI 紅 Kyoto University Research Information Repository

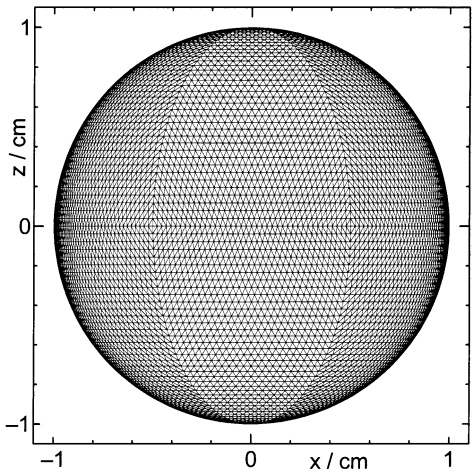

Fig. 1. Mesh pattern of a spherical dielectric with 19 200 elements.

IV. FMM

Detailed explanations of the FMM have appeared in many papers, such as [1], [2], and [4]–[6], so here we merely summarize the main features of the utilized FMM. The octree cell structure is defined so as to divide the points composed of the M node points and representative points of the boundary elements. The leaf cells have different sizes corresponding to the sizes of the enclosing elements, where no element sticks out from the convergence sphere of the leaf. The multipole and local expansions are represented by the pseudo-particle method [5], which offers one of the simplest sets of the formulae needed to code the FMM. The nearest neighbor list includes the second-nearest neighbors [2], so that the interactions via multipole expansions are separated by at least two intervening cells of the same size. The interaction list [2] of one leaf contains: 1) its neighbor leaves; 2) the neighbor leaves of its ancestor branches; and 3) some descendant leaves of its neighbor branches. The choice of 3) is judged by the Barnes and Hut algorithm [7]. The components of A_{near} are gathered according to the interaction list, although the list itself is not stored in memory.

V. Electrostatic Field Calculation by FMM-BEM

A. Parameter Setting

We have carried out a benchmark calculation by the FMM-BEM, concerning a dielectric sphere in vacuum under a uniform applied electrostatic field parallel to the z axis. The radius, relative permittivity, and field strength are 1 cm, 10 kV/cm, and 1 kV/cm, respectively. The spherical surface is divided into 19 200 curved triangular patches [8], as shown in Fig. 1. The u and D_n/ε_0 are each represented by a quadratic function on each patch, with 38 402 unknowns, thus resulting in a total of $N = 76\,804$.

We have calculated this example in three ways:

- case (a), without a precondition;
- case (b), with a precondition based on (2);
- case (c), with a precondition based on (1).

Table I summarizes the matrix used in each case. Case (a) is a standard composition that utilizes a stored A_{near} to save its repeating calculation. The size of ${A_{\mathrm{near}}}^{\mathrm{str}}$ is about 300 N for this example. Case (b) is a minimum memory composition that does not store the fairly large A_{near}. Case (c) is the most rapid composition, with the same amount of memory as in case (a). In cases (b) and (c), the minor loops require the DP calculation except for the ${A_{\mathrm{near}}}^{\mathrm{str}}$.

TABLE I
Composition of the Utilized Matrices

Case	Major loop	Minor loop
(a)	$A_{\mathrm{near}}^{\mathrm{str}} + A_{\mathrm{far}}$	not used
(b)	$A_{\mathrm{near}} + A_{\mathrm{far}}$	$A_{\mathrm{near}}^{\mathrm{DP}} + A_{\mathrm{far}}^{\mathrm{DP}}$
(c)	$A_{\mathrm{near}}^{\mathrm{str}} + A_{\mathrm{far}}$	$A_{\mathrm{near}}^{\mathrm{str}} + A_{\mathrm{far}}^{\mathrm{DP}}$

The major FMM requires a certain degree of precision, even if it results in a fairly slow calculation. On the other hand, the minor FMM requires sufficient speed even with a fairly low degree of precision. By considering this tradeoff relationship, we have employed eighth- and second-order expansions (both multipole and local) for the major and minor FMM, respectively. Furthermore, we judge the convergence of the major and minor Bi-CGSTAB2 methods by relative residual norms to be less than 10^{-8} and 10^{-5}, respectively.

In order to speed up the ${A_{\mathrm{near}}}^{\mathrm{DP}}$ calculation in case (b), we introduced the following measures.

- The partial components of A_{near} requiring singular integral calculations are stored in memory, the size of which is about 12 N ($\ll$ 300 N).
- The contributions from the second-nearest neighbors are calculated by the multipole expansion.
- The numerical integral formula of the triangular surface is fixed to the three-points formula.
- In the Barnes and Hut algorithm, the accuracy parameter θ [7] is reduced from 2.1 to 1.6 in order to increase the proportion of far parts.

B. Calculated Results

All the computations were performed on a PC with a Pentium IV 1.5-GHz single processor and 2 GB of RAM.

Fig. 2 shows the calculated potential and field on the z axis, plus the errors compared with the analytical true values. In all cases, the maximum error is observed around $z = 1$ cm, the "north pole" of the sphere. Although the errors are always less than $10^{-3}\%$, slight differences are observed among the three cases. These differences result from differences in the final converged state of the major iterative solver. These results show that our code is accurate enough for ordinary static field problems.

Fig. 3 shows the relative residual norms at the major iteration steps in relation to the calculation time. Case (a) requires 41 major steps and 24 708 s to converge. Cases (b) and (c) need three steps/7770 s and two steps/2458 s, respectively. The preconditioned major solvers need just a few steps. The total required times are 31.4% [case (b)] and 9.9% [case (c)] of case (a), although each step requires a longer time than that of case (a).

Fig. 4 shows the relative residual norms in relation to the iteration steps, where the results of minor loops are plotted for cases (b) and (c). The Bi-CGSTAB2 method calculates ${A_{\mathrm{appx}}}^{-1}\boldsymbol{b}_{\mathrm{arb}}$ twice through one major step. Thus, 3×2 and

京都大学 KYOTO UNIVERSITY
A Self-archived copy in
Kyoto University Research Information Repository
https://repository.kulib.kyoto-u.ac.jp
京都大学学術情報リポジトリ KURENAI 紅 Kyoto University Research Information Repository

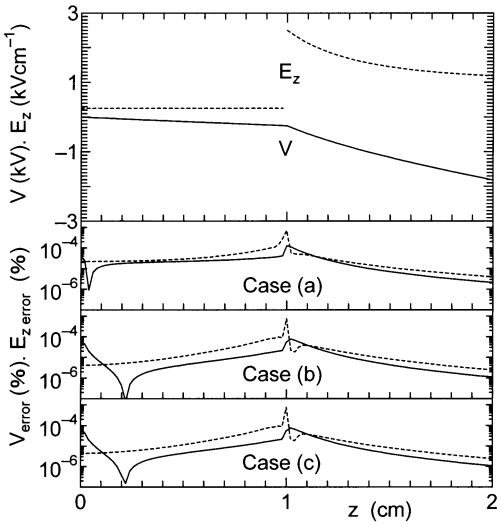

Fig. 2. Calculated potential and field on the z axis, plus their errors in cases (a), (b), and (c).

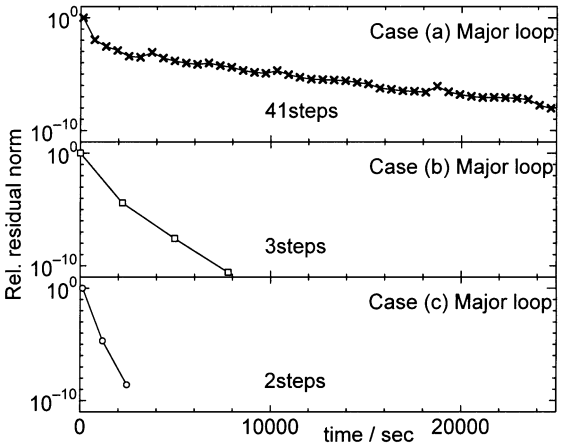

Fig. 3. Residual norm of the major iterative solver in relation to the calculation time.

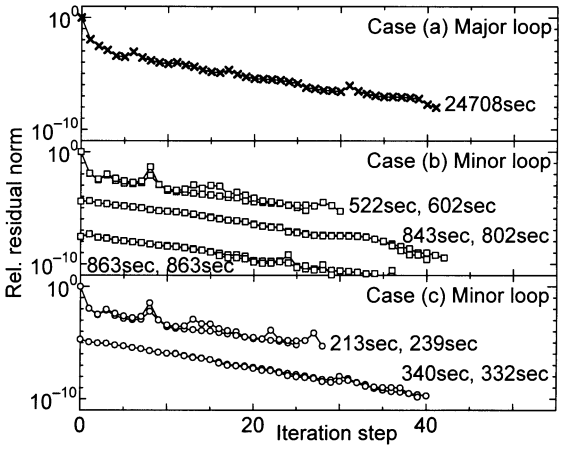

Fig. 4. Residual norm of the iterative solver in relation to the iteration step.

2×2 times of minor loops are required for cases (b) and (c), respectively. The minor loops show convergence tendencies similar to that of the major loop (a), but they need only

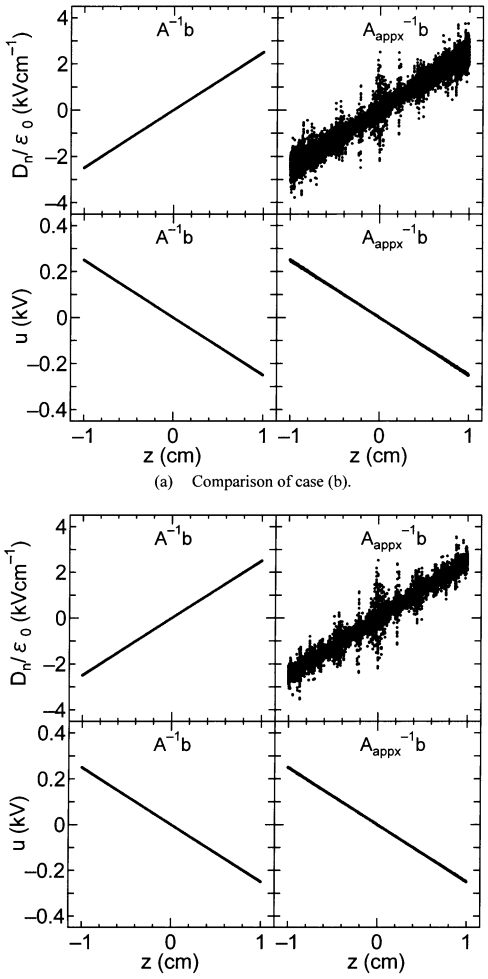

Fig. 5. Comparison of the $A^{-1}\boldsymbol{b}$ with the $A_{\mathrm{appx}}{}^{-1}\boldsymbol{b}$.

(b) 520-860 s and (c) 210-340 s, respectively, corresponding to (b) 2.1-3.5% and (c) 0.85-1.4% of the time needed for case (a).

The $\boldsymbol{x}_{\mathrm{appx}} = A_{\mathrm{appx}}{}^{-1}\boldsymbol{b}$ is compared with the $\boldsymbol{x} = A^{-1}\boldsymbol{b}$ in order to confirm the deteriorated precision of the DP-FMM, where $\boldsymbol{x} = (D_n/\varepsilon_0\, u)^T$. In Fig. 5, D_n/ε_0 and u are plotted in relation to the z axis, each with 38 402 points. Although the difference in u is quite small, that in D_n/ε_0 is noticeably large in both cases.

Fig. 6 shows the cumulative probabilities of the absolute values of these differences, $|A_{\mathrm{appx}}{}^{-1}\boldsymbol{b} - A^{-1}\boldsymbol{b}|$, taking values smaller than themselves. These curves clearly describe statistical properties of the differences, which are well fitted to the exponential distribution [9], $1 - \exp(-a|A_{\mathrm{appx}}{}^{-1}\boldsymbol{b} - A^{-1}\boldsymbol{b}|)$, where a is a parameter of the distribution function. Moreover, they obviously indicate the quality of A_{appx}, because it is clear that a better approximation is carried out when a curve stays at a leftward position in the figure. The differences in D_n/ε_0 and u at 97% probability are (b) 0.517 and 1.68 $\times 10^{-3}$, and (c) 0.404 and 9.12 $\times 10^{-4}$, respectively. Thus, the majority of D_n/ε_0 is roughly approximated by the DP-FMM. Therefore, the points having noticeable dispersion larger than 0.5 $kVcm^{-1}$ in Fig. 5 are composed of relatively few exceptional points having large burst errors. Fig. 6 also shows that the $A_{\mathrm{appx}}{}^{-1}\boldsymbol{b}$

京都大学 KYOTO UNIVERSITY
A Self-archived copy in
Kyoto University Research Information Repository
https://repository.kulib.kyoto-u.ac.jp
京都大学学術情報リポジトリ KURENAI 紅 Kyoto University Research Information Repository

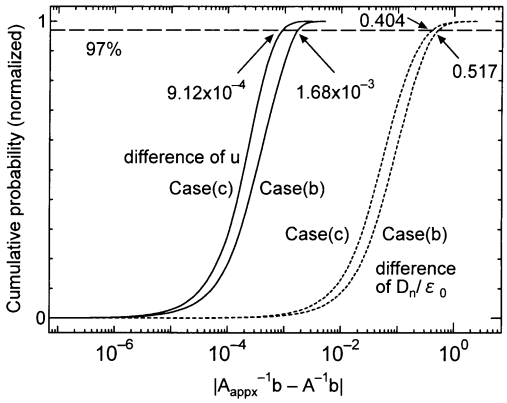

Fig. 6. Cumulative probability of the difference between the $A^{-1}\boldsymbol{b}$ and the ${A_{\rm appx}}^{-1}\boldsymbol{b}$.

of case (c) is better than that of case (b); this is because ${A_{\rm near}}^{\rm str}$ is more accurate than ${A_{\rm near}}^{\rm DP}$. This difference qualitatively explains the reason why case (c) needs fewer major steps than case (b) in Fig. 3.

Although we do not have sufficient space to describe practical calculation examples, we have already successfully applied this technique to many electrostatic field problems composed of complicated geometries. One of these examples is given in [10].

VI. Conclusion

We have proposed an effective precondition technique for the FMM, in which the nested iterative solver and FMM are used. In order to confirm the effectiveness of the technique, we have carried out an electrostatic field calculation of a spherical dielectric by using an FMM-BEM. A preconditioned FMM-BEM with stored $A_{\rm near}$ shortens the calculation time to about one-tenth of that without precondition. Another preconditioned FMM-BEM without stored $A_{\rm near}$ speeds up calculation by about three times compared to that without precondition and conserves the memory needed for the ${A_{\rm near}}^{\rm str}$. The proposed simple precondition technique can be applied to many kinds of linear problems that use the FMM.

References

[1] V. Rokhlin, "Rapid solution of integral equations of classical potential theory," *J. Comput. Phys.*, vol. 60, pp. 187–207, 1983.
[2] L. Greengard and V. Rokhlin, "A new version of the fast multipole mehod for the Laplace equation in three dimensions," *Acta Numerica*, vol. 6, pp. 229–269, 1997.
[3] M. H. Gutknecht, "Variants of Bi-CGSTAB for matrices with complex spectrum," *SIAM J. Sci. Comput.*, vol. 14, pp. 1020–1033, 1993.
[4] T. Nishida and K. Hayami, "The economic solution of 3D BEM using the fast multipole method" (in Japanese), in *Proc. Conf. JSCES*, vol. 1, 1996, pp. 315–318.
[5] J. Makino, "Yet another fast multipole method without multipoles," *J. Comput. Phys.*, vol. 151, pp. 910–920, 1999.
[6] A. Buchau and W. M. Rucker, "Preconditioned fast adaptive multipole boundary-element method," *IEEE Trans. Magn.*, vol. 38, pp. 461–464, 2002.
[7] J. Barnes and P. Hut, "A hierarchical $O(N \log N)$ force-calculation algorithm," *Nature*, vol. 324, pp. 446–449, 1986.
[8] S. Hamada and T. Takuma, "Surface charge method using a triangular Bezier patch with a variable interior control point," in *Proc. 13th COMPUMAG*, 2001, pp. I-82–I-83.
[9] I. N. Bronshtein and K. A. Semendyayev, *Handbook of Mathematics*, 3rd ed. Berlin, Germany: Springer, 1997, pp. 603–607.
[10] S. Hamada, O. Yamamoto, S. Okabe, and T. Takuma, "Three-dimensional electric field calculation around creeping discharges with fine mesh patterns based on bitmap pictures of dust figures," in *Proc. 14th Int. Conf. Gas Discharges and Their Applications*, vol. 2, Liverpool, U.K., 2002, pp. 176–179.